



Are judgements of circularity local or global?

Robert F. Hess *, Yi-Zhong Wang, Steven C. Dakin

McGill Vision Research, Department of Ophthalmology, McGill University, Montreal, Québec, Canada H3A 1A1

Received 14 January 1999; received in revised form 17 May 1999

Abstract

We assessed, in a task where subjects had to detect smooth deviations from circularity, whether the underlying mechanisms were localised in space to the size of the individual perturbations or whether they computed global shape. By manipulating the phase, the number of cycles of modulation and the spatial arrangement of the perturbations we argue that although either aspect can be detected, performance is ultimately limited by a global shape detecting mechanism. We show that this global mechanism receives input from spatially coarse, crossed orientationally tuned filters whose peak position in orientation depends on the overall shape to be detected. © 1999 Elsevier Science Ltd. All rights reserved.

Keywords: Circularity; Local; Global; Filtering; Orientation

1. Introduction

In principle, shape descriptions can be built up from single local estimates using filters matched to parts of objects or by more global estimates using large filters operating on the scale of the object as a whole. For example, a sinusoidally perturbed line (Fig. 1b) of the type used by Tyler (1973), when perturbed, contains energy at orientations (Fig. 1f) not present in the unperturbed stimulus. Orientationally selective cells in V1 tuned to orientations on either side of vertical would be ideal candidates to signal such a shape change. Such cells could operate on a very localised region of the stimulus. An alternative scheme but one which computes a real differences of localised peaks of the perturbation using non-oriented cells has also been suggested (Watt, Ward & Casco, 1987). On the other hand, the stimulus shown in Fig. 1d is a circular version of this. The unperturbed stimulus has energy at all orientations and when sinusoidally perturbed the energy at some orientations gets distributed. Now individual oriented cells responding over localised spatial regions are not going to be as sensitive in detecting these perturbations because it now becomes a pedestal

discrimination rather than a simple detection. Consequently one would expect sensitivity to be better for straight lines than for circles, but this is not the case (Wilkinson, Wilson & Habak, 1998).

This led Wilkinson et al. (1998) and Wilkinson and Wilson (1996) to postulate that the deformed circular patterns are processed in extrastriate cortex by specialised units composed of a polar arrangement of V1 orientationally tuned cells. According to such a scheme, perturbations from circularity are detected by orientationally selective cells feeding into a global mechanism responding over an area corresponding to the diameter of the circle. Such a mechanism adds up responses from oriented cells in a polar arrangement (Wilson, 1999). This suggestion followed on from the neurophysiological work of Gallant, Braun and Van Essen (1993) and Gallant, Connor, Rakshit, Lewis and Van Essen (1996) where they show evidence for cells in V4 having polar rather than Cartesian receptive field organisation.

In this study we ask two questions. First, ‘are deformations to circular D4 patterns detected by local or global shape mechanisms?’ and second, ‘what types of filtering operations are involved?’. Although we show evidence for both local and global processes, optimal sensitivity appears to be set by a global shape process. The filtering operations underlying our sensitivity to this task involve the comparison of sets of orthogonally oriented filter outputs operating over large spatial re-

* Corresponding author. Tel.: +1-514-843-1690; fax: +1-514-843-1691.

E-mail address: rhess@bradman.vision.mcgill.ca (R.F. Hess)

gions corresponding to the diameter of the circular stimulus.

2. Methods

2.1. Stimulus

Stimuli were circular 4th derivative of Gaussian (D4) contours (Wilkinson & Wilson, 1996), which are band-limited in spatial frequency domain (see Fig. 1). The circular D4 (later referred to as CD4 patterns) is generated by the following equations:

$$CD4 = L_m[1 + c(1 - 4r^2 + 4/3(r^4))e^{-r^2}] \quad (1)$$

$$r = \frac{\sqrt{x^2 + y^2} - R}{\sigma} \quad (2)$$

$$\sigma = \frac{\sqrt{2}}{\pi\omega_p} \quad (3)$$

σ is the space constant of D4. ω_p is the D4 peak spatial frequency. R is the radius of circular D4 contour, which is modulated sinusoidally according to the following formula

$$R = R_m\{1 + A \sin[f_r \arctan(y/x) + \theta]\} \quad (4)$$

where R_m is the mean radius; f_r is the radial frequency; A is the amplitude of the radial modulation, and θ is the phase of the modulation. $0 \leq \theta < 2\pi$.

Stimuli were generated digitally in MATLAB (MathWorks, Inc.) and displayed on a gamma-corrected, Macintosh gray-scale monitor using the Psychophysics Toolbox (Brainard, 1997) which provides high level access to the C-language VideoToolbox (Pelli, 1997). The mean luminance of the monitor was 20 cd/m². The stimulus screen subtended $12 \times 9^\circ$ at the viewing distance of 1.5 m. The mean radius was 0.5° . The radial frequencies were 4, 6, or 8 cyc/360° (see Fig. 2 for examples). The phase of radial modulation was 0, 90, 180, or 270°. The D4 peak spatial frequency was 5 cyc/deg. The contrast of stimuli was 80%.

2.2. Psychophysical procedures

A 2-interval, forced-choice paradigm was employed to estimate the detection thresholds of radial frequency modulations. One interval in a trial contained an unmodulated circular D4 contour and the other contained a modulated circular D4 contour. Subjects were asked to indicate which interval had the modulated (or non-circular) contour.

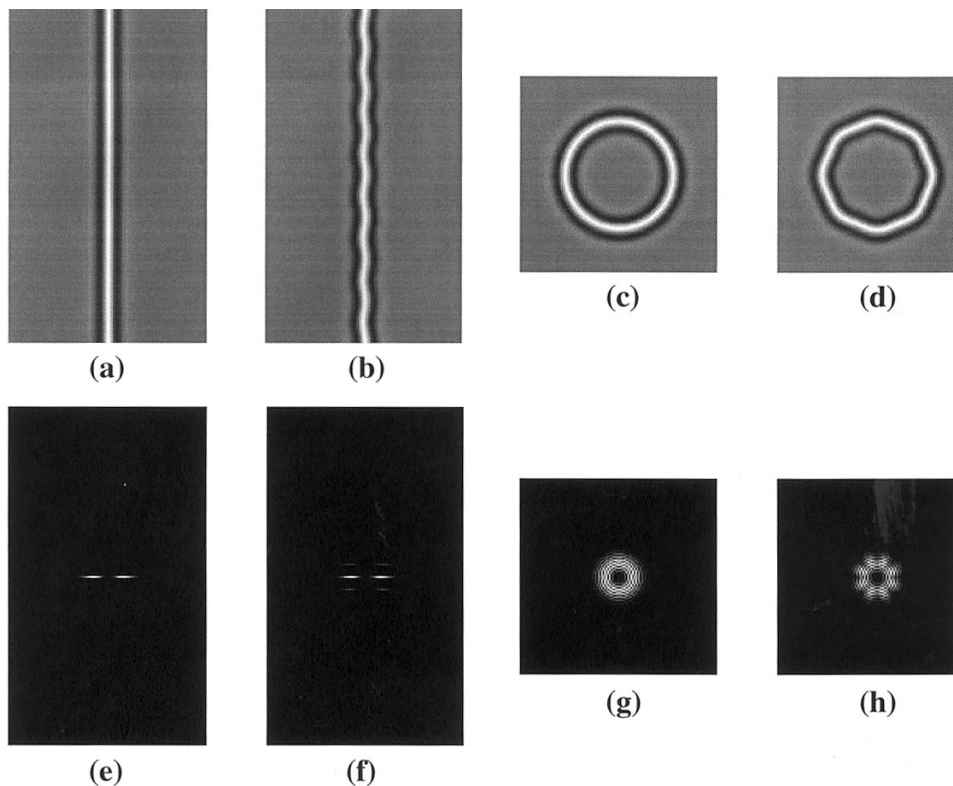


Fig. 1. Examples of sinusoidally modulated linear and circular D4 stimuli and their amplitude Fourier spectra. (a and b) An unmodulated and modulated linear D4 contour; (c and d) an unmodulated and modulated circular D4 contour. (e and f) The Fourier spectra of (a) and (b). (g and h) The Fourier spectra of (c) and (d). The mean radius, 35 pixels; amplitude modulation, 2%; modulation frequency, 8 cyc/360°; and modulation phase, 90°. The length of linear D4 is equal to the circumference of circular D4.

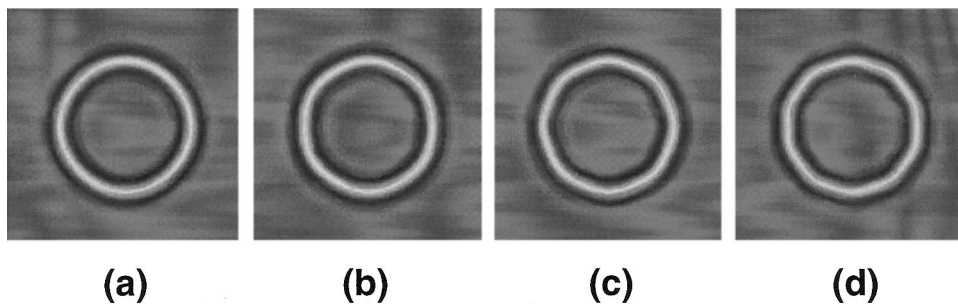


Fig. 2. Examples of stimuli used in this study. At viewing distance of 1.5 m, the D4 peak spatial frequency is 5 cyc/deg the mean radius is 0.5° . The amplitude of radial modulation is 1%. Radial frequencies are 4 (a), 6 (b), 8 (c), and 10 (d) cyc/360°, and the modulation phases are 90, 270, 90, and 270°, respectively.

The location of the stimulus presented on the screen was varied from trial to trial. The positional jittering of the stimulus presentation was introduced by adding Gaussian noise to the centring of the stimulus. The standard deviation of the Gaussian noise was equal to the mean radius of the circular D4 contour. The duration of each stimulus presentation was 0.5 s. Each session consisted of ten trials for each of five test modulations. Audio signals were used to prompt the subject just before and after each trial, but no feedback about the correctness of responses was provided. Psychometric functions of correct response versus test modulation were generated and fit with a Weibull function (Weibull, 1951; Nachmias, 1981). Threshold modulations corresponding to 82% correct were interpolated from the Weibull fits.

2.3. Number of cycles experiment

When the number of cycles of modulation was varied, the radial sinusoid was always terminated at a zero crossing. The probability summation prediction was computed in the following way. First, the empirical beta values from our psychometric functions were used to calculate the mean and standard deviation (S.D.) of the Weibull beta's. The mean was about 3 and S.D. was about 1. In the simulation, a beta value was drawn from a normal distribution with the empirical mean and S.D. To prevent getting extremely low thresholds predicted by probability summation, the beta value was not allowed to be lower than 1.7 which is the lowest beta found in the Weibull fitting of our experimental data. A mean threshold prediction which was the average of 7 independent predictions was obtained, each of which had a beta value drawn randomly from the normal distribution. This process mimics the seven runs in our experimental measurement. Instead of calculating S.E.M. of the mean prediction, the simulation computed the mean threshold prediction 100 times. Finally, The mean and 95% confidence limits of these 100 predictions were compared with the empirical data.

2.4. 'Pieces' experiment

First we generated circular D4 contours as usual. Then the CD4 contours were cut at a point of zero-crossing on the waveform into four pieces of equal size. Finally we re-arranged these four pieces in a regular row or randomly placed them in four quadrants to obtain the 'pieces' stimuli. The phase of the modulation was either fixed (data shown in Fig. 4) or randomly varied (data not displayed).

2.5. Filtering

First we generated a 2-D fractal noise array by weighting the amplitude spectrum of the uniformly distributed noise by one over spatial frequency ($1/f$). Then the fractal noise was filtered by orientational filters. For 4 cyc/360° radial frequency, a pair of orientational filters were used at the same time. For 6 cyc/360°, three orientational filters were used at the same time. The bandwidth of orientational filter was 20°. The centre of each orientational filter was chosen so that for 4 cyc/360°, noise orientations were around vertical and horizontal, or around 45 and 135° oblique; for 6 cyc/360°, noise orientations were around the axes which were either perpendicular or orthogonal to the sides of the deformed circular D4 patterns.

3. Results

3.1. Part 1 — local or global?

The first hint that sensitivity for these stimuli could be set by global shape rather than local features comes out of a comparison of thresholds for different phases of radial modulation for radial frequencies of 4 and 8 cyc/360°. These results are displayed in Fig. 3 for two subjects. Threshold sensitivity was better for phases of radial modulation of 90° and worse at both 0 and 180°, 270° was usually the worst. This is not expected of a purely local mechanism because these thresholds were

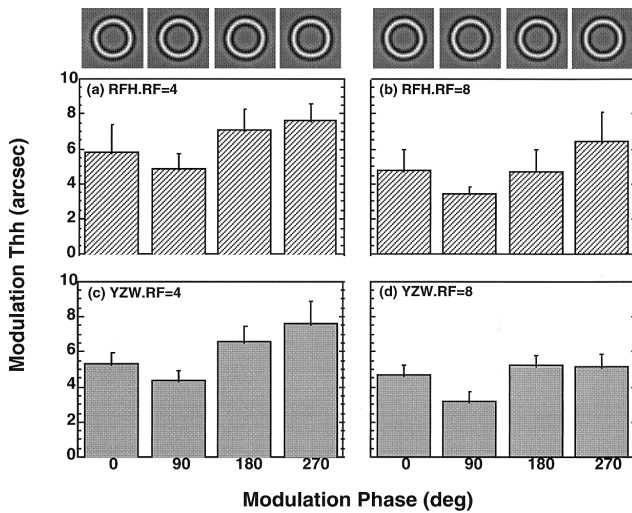


Fig. 3. Modulation thresholds for two subjects at two radial frequencies as a function of modulation phase. Best performance occurs at 90°, worst performance at 270°.

run in blocks where all stimuli were of one phase, the appearance of which (see figure insets) subjects had familiarised themselves with prior to and during testing.

Another way of addressing whether best performance is determined by a local or global mechanism is to assess how threshold detection varies with the number of cycles of radial modulation. For a local analysis, threshold detection should be just as good for a one stimulus cycle as it is for many stimulus cycles. It could be argued that there may be a probabilistic advantage of increasing the number of cycles for any purely local mechanism, although this would entail assumptions about the nature of the local analysis itself. Fig. 4 shows how threshold detection varies with the number of cycles of radial modulation for two subjects at two radial frequencies (4 and 8 cyc/360°). It is clear that

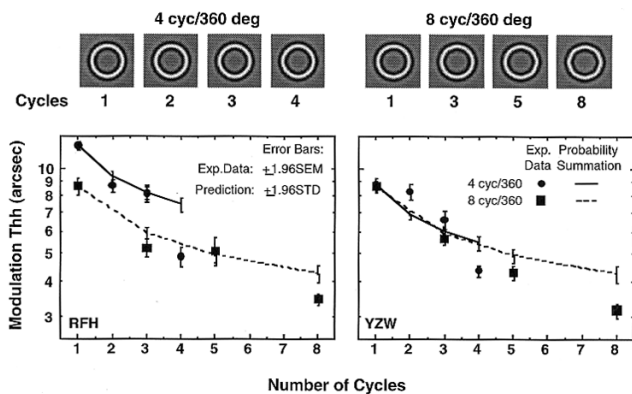


Fig. 4. Detection threshold ($\pm 95\%$ confidence limits) is plotted against the number of cycles of radial modulation for radial frequencies of 4 and 8 cyc/360°, for two subjects. The solid and dashed lines give the probability summation prediction ($\pm 95\%$ confidence limits, see Section 2) of a purely local mechanism which overestimates the terminal threshold in every case.

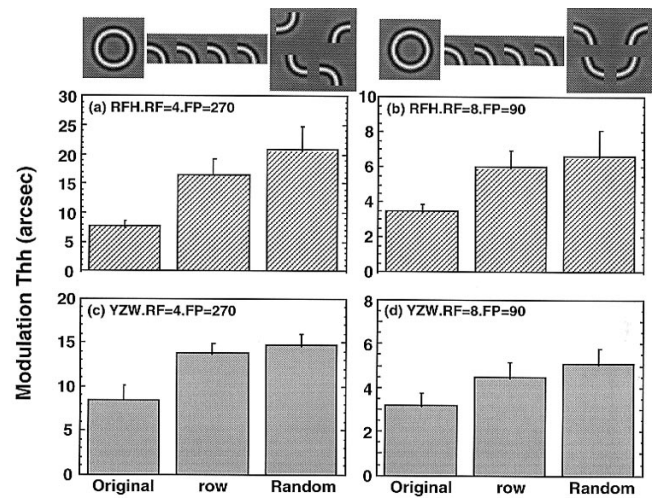


Fig. 5. Comparison of threshold performance for the detection of an intact circular D4 with regularly or randomly arranged pieces of the same stimulus. Performance is best for the intact stimulus suggesting a global shape mechanism.

thresholds decrease with the number of radial cycles. The solid and dashed lines are the probability summation predictions for 4 and 8 cyc/360°, respectively. The threshold advantage of a fully modulated stimulus runs counter to what one might expect of a purely local mechanism even if one resorts to the special pleading of probability summation. This is statistically significant ($P < 0.05$) for 4 as well as 8 cyc/360° for both subjects for the maximum cycle condition. This adds additional weight to the above suggestion that threshold for these patterns is set by a global rather than a local analysis.

A more direct test of the local/global distinction is to compare threshold sensitivity for radial D4 patterns with pieces of such patterns not arranged in a global shape. We used two arrangements of the pieces, one where they were arranged in a row and another where they were positioned at random (see Fig. 5 insets). In all three of these arrangements (circular, pieces in a row, pieces at random), the radial modulation which could be of 4 or 8 cyc/360° could also be of fixed or random spatial phase. The results are shown in Fig. 5. Modulation threshold is lowest for the circular D4, intermediate for its pieces arranged in a row and highest for its pieces arranged randomly. Since the same local information is present in all three conditions, if there is only a local mechanism present, performance should be comparable. The fact that it is better for the circular case argues for an underlying global process that utilises the overall shape information. We assume that the task is accomplished locally for the pieces and that this is why performance is further disrupted when the spatial phase of the modulations is randomised. It would seem therefore that both local and global processes can be used to solve this task with the global process having better sensitivity in the circular D4 case.

3.2. Part II — nature of the filtering operations

In order to understand the filtering properties of the mechanisms underlying the global shape detection of these patterns we measured threshold sensitivity in the presence of luminance noise. The stimulus was either embedded in the noise (Fig. 6a and c) such that noise surrounded the stimulus but did not overlap it, or added to it (Fig. 6b and d) so that it overlaid and surrounded it. The former has the advantage of not affecting any global mechanism that restricts its operation to just the circular stimulus, for example a mechanism whose weighting function excludes all but the circular region of the stimulus. On the other hand if circularity is determined by a mechanism working at the scale of the circle (i.e. summing over the whole stimulus including the inner area bordered by the circle) then embedded noise will have a significant effect. Thus such a comparison of the masking produced by embedded and additive noise bears upon the spatial integration of any global shape mechanism. The main results are shown in Fig. 6 where we compare the detection of a 4 cyc/360° (phase, 90°), circular D4 pattern without noise and with two types of oriented noise; cross oblique and cross horizontal/vertical.

In both embedded and additive cases, horizontal/vertical noise has little effect on performance whereas oblique noise does impair performance. The fact that there is masking at all in the embedded case suggests that the global weighting function of the underlying mechanism extends beyond the stimulus itself. Information in the adjacent regions to the stimulus must also be used. That oblique noise not horizontal/vertical noise is effective in masking performance for this 4 cyc/360° D4

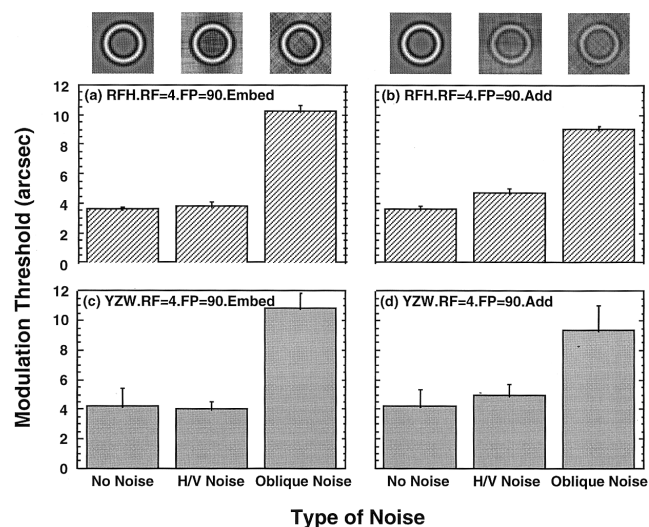


Fig. 6. Comparison of threshold performance for a 4 cyc/360°, D4 pattern (phase, 90°) embedded in or added to spatial noise of crossed orientation (horizontal/vertical or oblique). Oblique noise disrupts threshold.

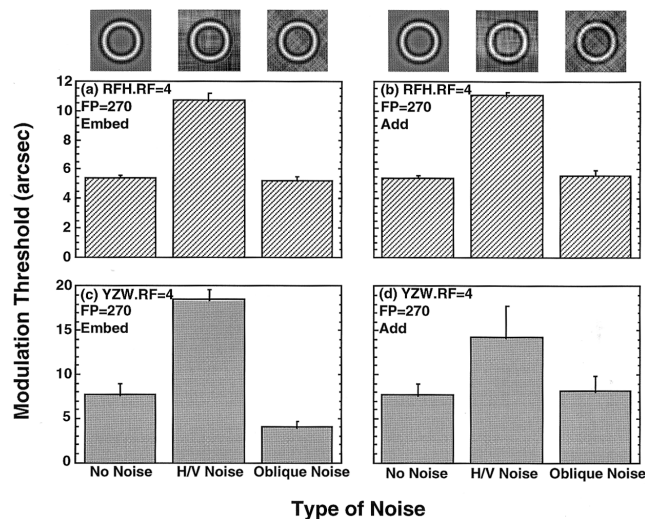


Fig. 7. Comparison of threshold performance for a 4 cyc/360°, D4 pattern (phase, 270°) embedded in or added to spatial noise of crossed orientation (horizontal/vertical or oblique). Horizontal/vertical noise disrupts threshold.

stimulus set at 90° phase suggests that performance is determined by a mechanism that has input from only one set of orthogonally oriented filters.

There are a number of implications of this result. Deviations from circularity may not be detected by unitary mechanisms that simply sum across a wide range of orientations (Wilson, 1999). Such a mechanism would be equally affected by the two cross orientation masking conditions. It would seem that the underlying mechanism involves only a comparison of the output of orthogonally oriented filters. The number and position of which depend on the radial frequency and its phase respectively. A population of detectors each summing individual orientations in a polar manner (Wilkinson et al., 1998) may offer a plausible explanation.

We now address two additional but related questions. First, are the filters whose outputs are compared (e.g. the oblique filters in the results shown in Fig. 6) fixed or do they depend on the phase of the radial modulation? Second, if the active filters depend on the phase of the radial modulation, are they oriented parallel or orthogonal to the sides of the modulated stimulus? Fig. 7 displayed comparable data to that already described in Fig. 6 but now the 4 cyc/360° CD4 stimulus is at 270° phase (i.e. a square) rather than 90° phase (i.e. the diamond). Now the results of Fig. 7 show that the effective noise is that oriented horizontally and vertically and not obliquely as in Fig. 6. This shows that the effective filters depend on the global shape of the stimulus (e.g. in this case a diamond versus a square) and that it is the sides of the figure rather than its corners that are important for this shape discrimination.

However, it is still ambiguous in this case (i.e. 4 cyc/360° CD4) whether noise parallel to or orthogonal to the sides of the distorted circle are relevant. The results displayed in Fig. 8 which are for a 6 cyc/360° CD4 pattern (phase, 90°) for noise (three oriented bandlimited filters, 20° bandwidth) parallel and orthogonal to the sides help to resolve this question because now we can arrange the noise to be either parallel to or orthogonal to the sides of the global shape. The results show that it is the noise parallel to the sides of the pattern that is most disruptive. Noise orthogonal to the sides is either not effective at all or produces a slight enhancement of threshold sensitivity.

4. Discussion

Sinusoidal radial modulations to circular D4 patterns produce both local and global deformation. For frequencies of 4 and 8 cyc/360°, it would appear to be the global shape changes that determine our detection performance. First, performance depends on the absolute phase which determines the overall shape of the stimulus. Second, performance is better than the probability summation prediction when the number of radial cycles is varied. Third, performance is better when the modulations are part of a circular structure than when they are presented separately.

This conclusion is consistent with two previous studies. Wilkinson et al. (1998) have shown that the contrast response function for detecting sinusoidal modulations in a straight line and a circle are different. The former has a much stronger dependence on contrast. Secondly, the predictions (relationship between modulation sensitivity and radial frequency) of two

candidate local cues, namely local orientation (slope of -1) and local curvature (slope of -2) are not met. Keeble and Hess (1999) showed that the discrimination of perturbations in circularity for Gabor micropatterns is not affected by the form of the probability density function of the spatial jitter. This suggests that performance is governed by the integration of spatial information rather than the detection of outliers.

In principle, any putative global mechanism could involve the integration of local oriented filters just corresponding to the circular stimulus or large filters summing over the circle as a whole (Fig. 8). The fact that oriented embedded noise disrupts performance but that the disruption is less than that for additive noise suggests that the underlying spatial weighting function extends beyond the stimulus area. The masking results suggests that there must be arrays of detectors comprising different numbers and orientations of orthogonally arranged filters to encode the shape changes measured here. Higher radial frequencies require detectors with correspondingly larger number of oriented subunits. Whether this extends beyond 6 cyc/360° (see Wilkinson et al., 1998) is at present unknown.

4.1. Edges versus sides

In principle deviations from circularity can be signalled either by the emergence of corner features or straight sides within a global analysis. In terms of what we know of the neurophysiology, end-stopped cells could form the subunits of a global detector for the former and simple cells, the subunits of a global detector for the latter (Hubel & Wiesel, 1968). Recently, a case has been made for both the role of end-stopped cells, (specifically the hypercomplex type II of Dreher, 1972), in contour corner analysis (Heitger, Rosenthaler, von der Heydt, Peterhans & Kubler, 1992). The masking results of this study suggest that it is not the corner features but the side features that are being globally encoded. This in turn suggests that the basic building block of a global ‘circularity’ detector may involve linear oriented filters (for example, simple cells) arranged in a polar fashion. Just how their outputs are combined is as yet unknown.

4.2. Models

Although the original proposal put forward by Wilson (1999) concerning a unitary detector with oriented subunits may not form an explanation for these results, its later elaboration in terms of a population code (Wilkinson et al., 1998) in which the outputs of a number of orientationally selective units are compared may be able to account for the orientationally selective masking results reported here.

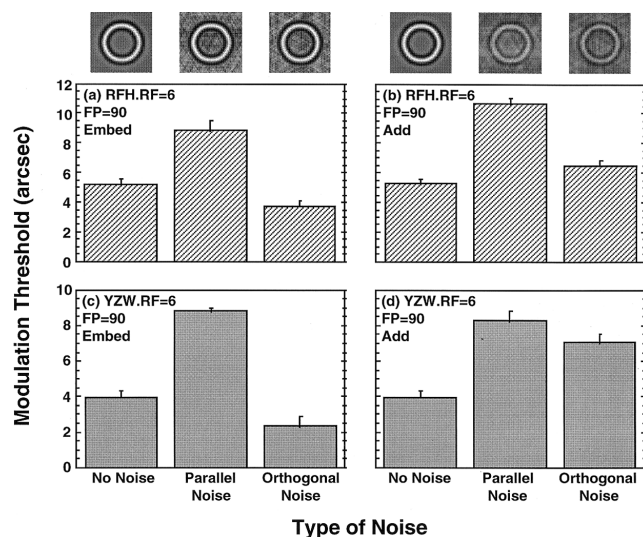


Fig. 8. Comparison of threshold performance for a 6 cyc/360°, D4 pattern (phase, 90°) embedded in or added to spatial noise of crossed orientation (parallel or orthogonal). Parallel noise disrupts threshold.

Acknowledgements

This work was supported by a grant from the Medical research Council of Canada MT-10818.

References

- Brainard, D. H. (1997). The Psychophysics Toolbox, *Spatial Vision*, 10, 433–446.
- Dreher, B. (1972). Hypercomplex cells in cat's striate cortex. *Ophthalmology*, 11, 355–356.
- Gallant, J. L., Braun, J., & Van Essen, D. C. (1993). Selectivity for polar, hyperbolic, and Cartesian gratings in macaque visual cortex. *Science*, 259, 100–103.
- Gallant, J. L., Connor, C. E., Rakshit, S., Lewis, J. W., & Van Essen, D. C. (1996). Neural responses to polar, hyperbolic, and Cartesian gratings in area V4 of the macaque monkey. *Journal of Neurophysiology*, 76, 2718–2739.
- Heitger, F., Rosenthaler, L., von der Heydt, R., Peterhans, E., & Kubler, O. (1992). Simulation of neural contour mechanisms: from simple to end-stopped cells. *Vision Research*, 32, 963–981.
- Hubel, D. H., & Wiesel, T. N. (1968). Receptive fields and functional architecture of monkey striate cortex. *Journal of Physiology*, 195, 215–243.
- Keeble, D., & Hess, R.F. (1999). Discriminating local continuity in curved figures. *Vision Research*, 39, 3287–3300.
- Nachmias, J. (1981). On the psychometric function for contrast detection. *Vision Research*, 21, 215–223.
- Pelli, D. G. (1997). The VideoToolbox software for visual psychophysics: transforming numbers into movies. *Spatial Vision*, 10, 437–442.
- Tyler, C. W. (1973). Periodic vernier acuity. *Journal of Physiology (London)*, 228, 637–647.
- Watt, R. J., Ward, R. M., & Casco, C. (1987). The detection of deviation from straightness in lines. *Vision Research*, 27, 1659–1678.
- Weibull, W. (1951). A statistical distribution function of wide applicability. *Journal of Applied Mechanics*, 18, 292–297.
- Wilkinson, F., & Wilson, H. R. (1996). Discrimination of curvilinear patterns: Beyond simple cells. *Investigative Ophthalmology and Vision Science*, 37, S955.
- Wilkinson, F., Wilson, H. R., & Habak, C. (1998). Detection and recognition of radial frequency patterns. *Vision Research*, 38, 3555–3568.
- Wilson, H. R. (1999). Non-fourier cortical processes in texture, form and motion perception. In P. S. Ulinski, & E. G. Jones, *Cerebral cortex*. In: *Models of cortical circuitry*, vol. 13 (pp. 445–477). New York: Plenum Press.